Supporting Information

Dual emissive Ln(III)–Ag(I) heterometallic chains based on tris(2-pyridyl)phosphine oxide

Yuliya A. Bryleva,[1] Mariana I. Rakhmanova, Alexander V. Artem'ev, Andrey Yu. Baranov, and Ludmila A. Glinskaya

Nikolaev Institute of Inorganic Chemistry, Siberian Branch of the Russian Academy of Sciences, 3, Academician Lavrentiev Avenue, Novosibirsk 630090, Russian Federation

[1]*Corresponding author*

E-mail address: bryleva@niic.nsc.ru (Yu. A. Bryleva)

Contents

Table S1. Selected bond lengths and angles for **2**·3MeCN and **3**·3MeCN.

2·3MeCN				**3**·3MeCN			
Bond	Bond length (Å)	Bond	Bond length (Å)	Bond	Bond length (Å)	Bond	Bond length (Å)
Eu1–O1	2.363(4)	Ag1–N1A^{iii}	2.494(7)x2	Tb1–O1	2.334(3)	Ag1–N1A^{ii}	2.482(5)x2
Eu1–O2	2.354 (4)	Ag1–N1B^{iii}	2.468(7)x2	Tb1–O2	2.327(3)	Ag1–N1B^{ii}	2.473(5)x2
Eu1–O11	2.450(5)	Ag1–N1C^{iii}	2.487(7)x2	Tb1–O11	2.425(3)	Ag1–N1C^{ii}	2.484(5)x2
Eu1–O12	2.504(5)	Ag2–N1D^{i}	2.503(7)x2	Tb1–O12	2.481(4)	Ag2–N1D^{i}	2.504(5)x2
Eu1–O21	2.516(7)	Ag2–N1E^{i}	2.412(6)x2	Tb1–O21	2.491(8)	Ag2–N1E^{i}	2.407(5)x2
Eu1–O22	2.510(6)	Ag2–N1F^{i}	2.647(8)x2	Tb1–O21'	2.535(11)	Ag2–N1F^{i}	2.665(6)x2
Eu1–O31	2.507(9)	Ag3–N1G	2.525(6)	Tb1–O22	2.504(11)	Ag3–N1G^{iii}	2.522(4)
Eu1–O31'	2.505(15)	Ag3–N1H	2.455(7)	Tb1–O22'	2.509(13)	Ag3–N1H^{iii}	2.456(5)
Eu1–O32	2.492(9)	Ag3–N1I	2.473(7)	Tb1–O31	2.486(7)	Ag3–N1I^{iii}	2.469(5)
Eu1–O32'	2.520(16)	Ag3–N1J^{ii}	2.529(7)	Tb1–O31'	2.485(11)	Ag3–N1J	2.539(5)
Eu1–O41	2.557(7)	Ag3–N1K^{ii}	2.518(7)	Tb1–O32	2.476(7)	Ag3–N1K	2.509(5)
Eu1–O42	2.516(6)	Ag3–N1O^{ii}	2.445(7)	Tb1–O32'	2.477(12)	Ag3–N1O	2.445(5)
Eu2–O3	2.351(4)			Tb1–O41	2.547(5)		
Eu2–O4	2.361 (4)			Tb1–O42	2.496(5)		
Eu2–O51	2.488(7)			Tb2–O3	2.327(3)		
Eu2–O52	2.539(6)			Tb2–O4	2.331(3)		
Eu2–O61	2.488(10)			Tb2–O51	2.473(5)		
Eu2–O61'	2.525(12)			Tb2–O52	2.521(5)		
Eu2–O62	2.533(10)			Tb2–O61	2.472(7)		
Eu2–O62'	2.514(13)			Tb2–O61'	2.504(10)		
Eu2–O71	2.549(11)			Tb2–O62	2.521(7)		
Eu2–O71'	2.527(12)			Tb2–O62'	2.491(11)		
Eu2–O72	2.546(13)			Tb2–O71	2.499(10)		
Eu2–O72'	2.549(14)			Tb2–O71'	2.519(15)		
Eu2–O81	2.474(5)			Tb2–O72	2.512(11)		
Eu2–O82	2.495(5)			Tb2–O72'	2.529(15)		
				Tb2–O81	2.445(4)		
				Tb2–O82	2.469(4)		

Angle	Angle size (°)	Angle	Angle size (°)	Angle	Angle size (°)	Angle	Angle size (°)
O1–Eu1–O11	76.7(2)	N1B–Ag1–N1C	79.4(3)x2	O1–Tb1–O11	77.0(2)	N1A–Ag1–N1C	83.6(2)x2
O1–Eu1–O12	74.7(2)	N1B^{iii}–Ag1–N1C	94.9(2)x2	O1–Tb1–O12	74.8(2)	N1A–Ag1–N1C^{ii}	100.9(2)x2
O1–Eu1–O21	69.3(2)	N1B^{iii}–Ag1–N1A	177.0(2)x2	O1–Tb1–O21	71.2(4)	N1A^{ii}–Ag1–N1A	101.4(2)
O1–Eu1–O22	114.1(2)	N1B–Ag1–N1A	82.4(2)x2	O1–Tb1–O21'	66.5(3)	N1B–Ag1–N1A	82.1(2)x2
O1–Eu1–O31	81.2(2)	N1C–Ag1–N1A	83.5(2)x2	O1–Tb1–O22	112.5(5)	N1B–Ag1–N1A^{ii}	176.5(2)x2
O1–Eu1–O31'	82.0(4)	N1C^{iii}–Ag1–N1A	101.9(2)x2	O1–Tb1–O22'	116.7(3)	N1B–Ag1–N1C	79.7(2)x2
O1–Eu1–O32	128.5(3)	N1A–Ag1–N1A^{iii}	100.4(3)	O1–Tb1–O31	81.4(2)	N1B–Ag1–N1C^{ii}	95.5(2)x2
O1–Eu1–O41	69.8(2)	N1B^{iii}–Ag1–N1B	94.8(3)	O1–Tb1–O31'	82.2(3)	N1B^{ii}–Ag1–N1B	94.4(2)
O1–Eu1–O42	118.1(2)	N1C–Ag1–N1C^{iii}	171.7(4)	O1–Tb1–O32	129.1(2)	N1C^{ii}–Ag1–N1C	173.0(3)
O1–Eu1–O2	148.3(2)	N1D^{i} –Ag2–N1F	106.3(2)x2	O1–Tb1–O32'	130.2(3)	N1D–Ag2–N1F	85.9(2)x2
O2–Eu1–O11	77.0(2)	N1E–Ag2–N1D^{i}	172.5(3)x2	O1–Tb1–O41	69.4(2)	N1D–Ag2–N1F^{i}	106.8(2)x2
O2–Eu1–O12	75.2(2)	N1D^{i}–Ag2–N1F^{i}	85.6(2)x2	O1–Tb1–O42	117.9(2)	N1D^{i}–Ag2–N1D	91.8(2)
O2–Eu1–O21	116.4(2)	N1E–Ag2–N1D	82.7(2)x2	O2–Tb1–O1	148.4(1)	N1E–Ag2–N1D	82.7(1)x2
O2–Eu1–O22	67.6(2)	N1E–Ag2–N1F	78.1(2)x2	O2–Tb1–O11	76.7(1)	N1E–Ag2–N1D^{i}	172.5(2)x2
O2–Eu1–O31	130.3(3)	N1E–Ag2–N1F^{i}	91.4(2)x2	O2–Tb1–O12	75.3(3)	N1E–Ag2–N1F	77.9(2)x2
O2–Eu1–O31'	128.7(3)	N1D^{i}–Ag2–N1D	91.5(3)	O2–Tb1–O21	118.0(2)	N1E–Ag2–N1F^{i}	91.0(2)x2
O2–Eu1–O32	82.4(3)	N1E–Ag2–N1E^{i}	103.4(3)	O2–Tb1–O21'	113.4(5)	N1E^{i}–Ag2–N1E	103.3(2)
O2–Eu1–O32'	81.9(5)	N1F^{i}–Ag2–N1F	163.1(3)	O2–Tb1–O22	67.0(3)	N1F^{i}–Ag2–N1F	162.1(3)
O2–Eu1–O41	116.7(2)	N1O^{ii}–Ag3–N1I	101.5(3)	O2–Tb1–O22'	70.1(5)	N1G^{iii}–Ag3–N1J	175.2(2)
O2–Eu1–O42	70.1(2)	N1O^{ii}–Ag3–N1J^{ii}	79.2(2)	O2–Tb1–O31	129.9(2)	N1H^{iii}–Ag3–N1G^{iii}	78.7(2)
O3–Eu2–O51	69.4(2)	N1O^{ii}–Ag3–N1G	95.7(2)	O2–Tb1–O31'	128.5(3)	N1H^{iii}–Ag3–N1I^{iii}	81.9(1)
O3–Eu2–O52	117.0(2)	N1O^{ii}–Ag3–N1K^{ii}	82.2(2)	O2–Tb1–O32	81.8(2)	N1H^{iii}–Ag3–N1J	106.2(2)
O3–Eu2–O71	70.4(4)	N1O^{ii}–Ag3–N1H	173.0(3)	O2–Tb1–O32'	81.2(3)	N1H^{iii}–Ag3–N1K	93.9(2)
O3–Eu2–O71'	71.3(5)	N1I–Ag3–N1J^{ii}	96.8(2)	O2–Tb1–O41	116.8 (2)	N1I^{iii}–Ag3–N1G^{iii}	83.7(2)
O3–Eu2–O72	119.8(3)	N1I–Ag3–N1G	83.6(2)	O2–Tb1–O42	70.1(2)	N1I^{iii}–Ag3–N1J	96.9(2)
O3–Eu2–O72'	115.3(7)	N1I–Ag3–N1K^{ii}	175.0(2)	O3–Tb2–O4	148.3(1)	N1I^{iii}–Ag3–N1K	175.0(2)
O3–Eu2–O61	79.0(2)	N1G–Ag3–N1J^{ii}	174.8(3)	O3–Tb2–O51	69.4(2)	N1K–Ag3–N1G^{iii}	92.9(2)
O3–Eu2–O61'	80.2(3)	N1K^{ii}–Ag3–N1J^{ii}	87.1(2)	O3–Tb2–O52	116.5(2)	N1K–Ag3–N1J	86.8(2)
O3–Eu2–O62	125.5(3)	N1K^{ii}–Ag3–N1G	92.7(2)	O3–Tb2–O61	78.9(2)	N1O–Ag3–N1G^{iii}	96.0(2)
O3–Eu2–O62'	126.1(4)	N1H–Ag3–N1I	81.8(2)	O3–Tb2–O61'	80.0(3)	N1O–Ag3–N1H^{iii}	173.5(2)
O3–Eu2–O81	77.6(2)	N1H–Ag3–N1J^{ii}	106.7(2)	O3–Tb2–O62	125.2(2)	N1O–Ag3–N1I^{iii}	101.5(2)
O3–Eu2–O82	77.5(2)	N1H–Ag3–N1G	78.5(2)	O3–Tb2–O62'	126.8(3)	N1O–Ag3–N1J	79.1(2)
O3–Eu2–O4	148.2(2)	N1H–Ag3–N1K^{ii}	94.2(2)	O3–Tb2–O71	70.6(3)	N1O–Ag3–N1K	82.5(1)

O4–Eu2–O51	115.6(2)			O3–Tb2–O71'	70.9(4)		
O4–Eu2–O52	68.2(2)			O3–Tb2–O72	118.0(4)		
O4–Eu2–O61	132.1(3)			O3–Tb2–O72'	119.9(3)		
O4–Eu2–O61'	130.7(3)			O3–Tb2–O81	77.3(1)		
O4–Eu2–O62	85.9(3)			O3–Tb2–O82	77.1(1)		
O4–Eu2–O62'	85.4(3)			O4–Tb2–O51	116.3(2)		
O4–Eu2–O71	110.4(8)			O4–Tb2–O52	67.9(2)		
O4–Eu2–O71'	118.3(4)			O4–Tb2–O61	132.1(2)		
O4–Eu2–O72	70.5(3)			O4–Tb2–O61'	130.7(3)		
O4–Eu2–O72'	67.9(3)			O4–Tb2–O62	85.9 (2)		
O4–Eu2–O81	73.9(2)			O4–Tb2–O62'	84.6(3)		
O4–Eu2–O82	74.1(2)			O4–Tb2–O71	116.6(6)		
				O4–Tb2–O71'	108.7(6)		
				O4–Tb2–O72	67.5(3)		
				O4–Tb2–O72'	71.7(5)		
				O4–Tb2–O81	74.4(1)		
				O4–Tb2–O82	74.6(1)		

2·3MeCN: Symmetry code(s): (i) *x*, -*y*+1, -*z*+1; (ii) -*x*+1/2, *y*+1/2, -*z*+3/2; (iii) -*x*+3/2, *y*-1/2, -*z*+3/2; (iv) -*x*+3/2, *y*+1/2, -*z*+3/2.
3·3MeCN: Symmetry code(s): (i) *x*, -*y*, -*z*+1; (ii) *x*, -*y*+1, -*z*+1; (iii) *x*, -*y*+2, -*z*+1; (iv) -*x*+1/2, *y*-1/2, -*z*+3/2.

Table S2. Unit cell parameters of CPs (**1**–**4**)·3MeCN measured at 150 K.

Compound	***a*, Å**	***b*, Å**	***c*, Å**	***α*, °**	***β*, °**	***γ*, °**	***V*, Å^3**
1·3MeCN	16.07	29.12	38.91	90	90	90	18203
2·3MeCN	16.06	29.10	38.55	90	90	90	18015
3·3MeCN	16.07	28.93	38.86	90	90	90	18060
4·3MeCN	16.11	28.87	38.90	90	90	90	18089

Table S3. The room-temperature photoluminescence lifetimes of CPs **1**–**4** before (τ_1) and after (τ_2) irradiation at 312 nm for 3 hours. The lifetimes were measured by monitoring the emission lines of Sm^{3+} ($^4G_{5/2}\rightarrow{}^6H_{9/2}$), Eu^{3+} ($^5D_0\rightarrow{}^7F_2$), Tb^{3+} ($^5D_4\rightarrow{}^7F_5$), and Dy^{3+} ($^4F_{9/2}\rightarrow{}^6H_{13/2}$) ions at λ_{ex} = 320 nm**.**

Compound	**1**	**2**	**3**	**4**
τ_1**, µs**	90	777	772	56
τ_2**, µs**	96	801	796	59

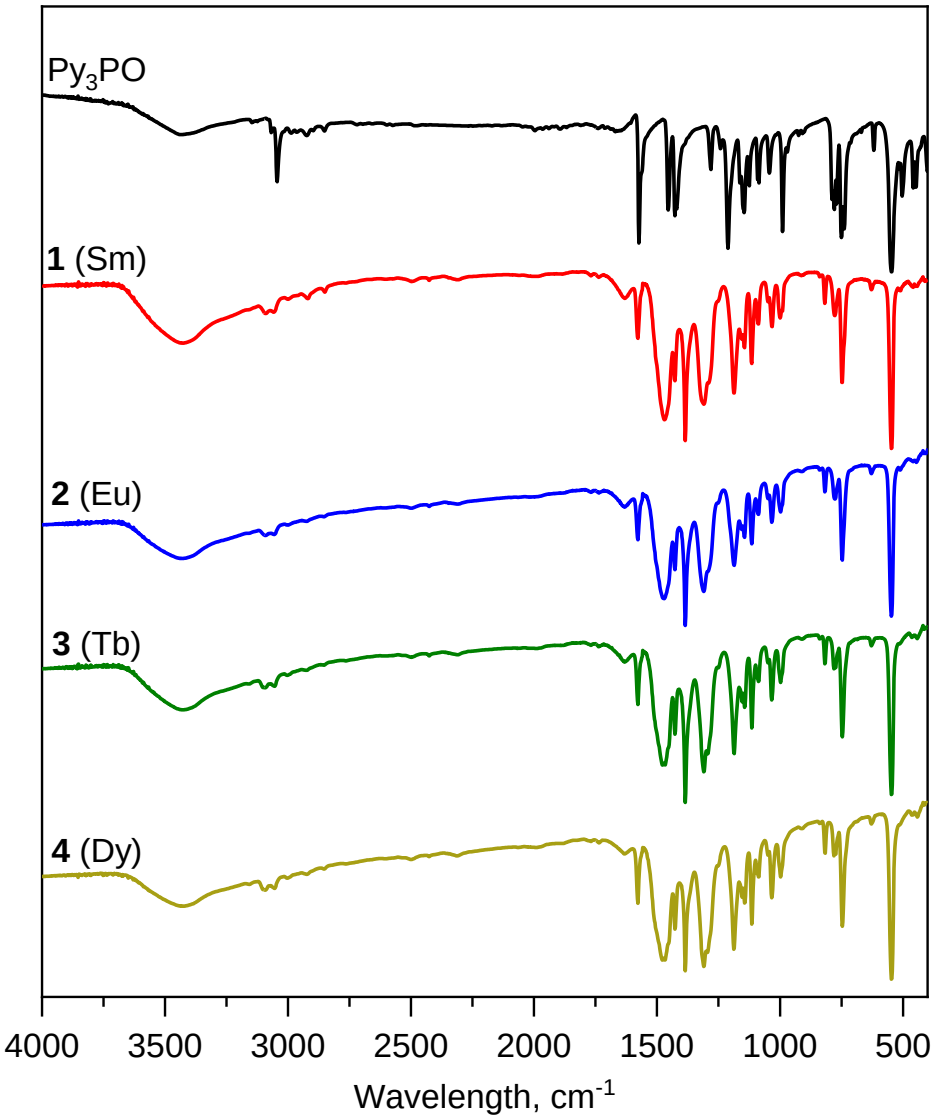

Figure S1. FT-IR spectra of Py_3PO and CPs **1**–**4**.

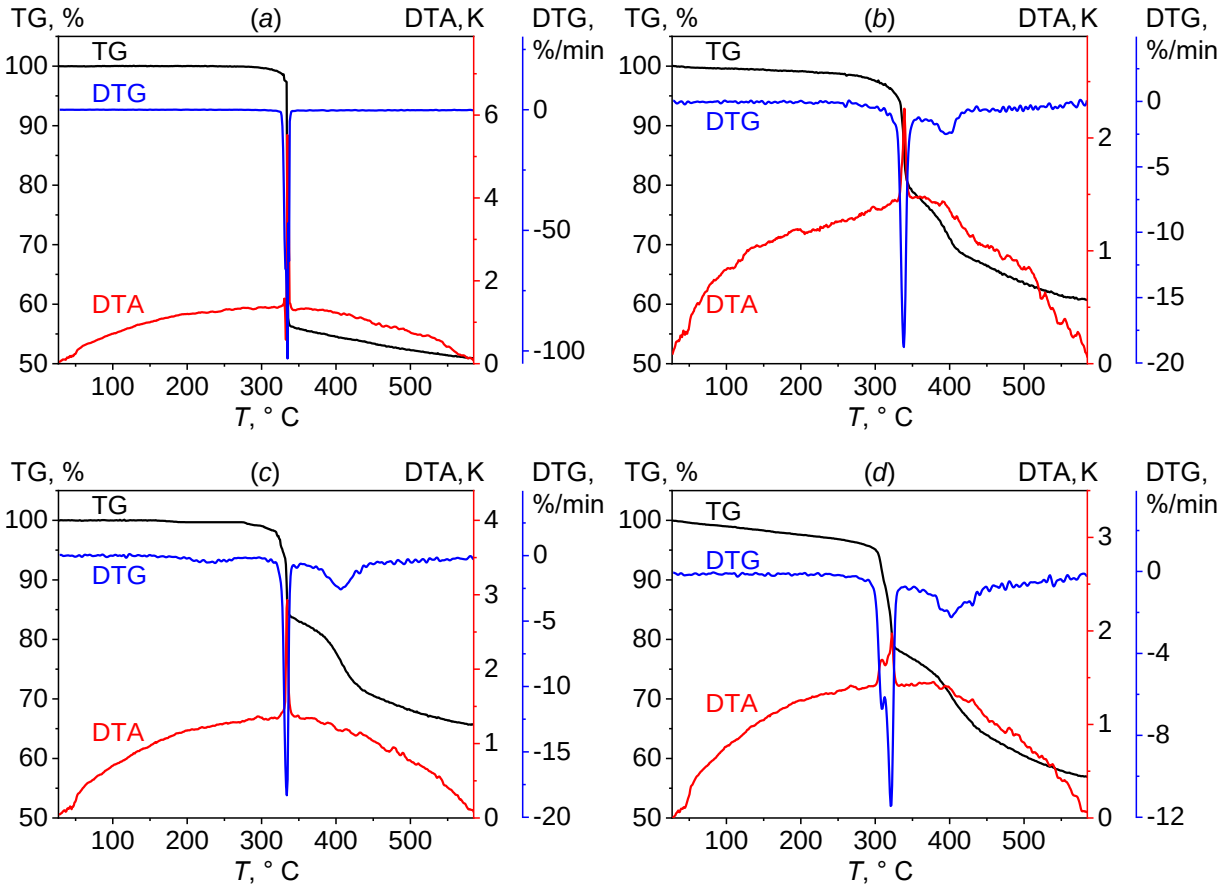

Figure S2. TG, DTA, and DTG of CPs **1** (*a*), **2** (*b*), **3** (*c*), and **4** (*d*).

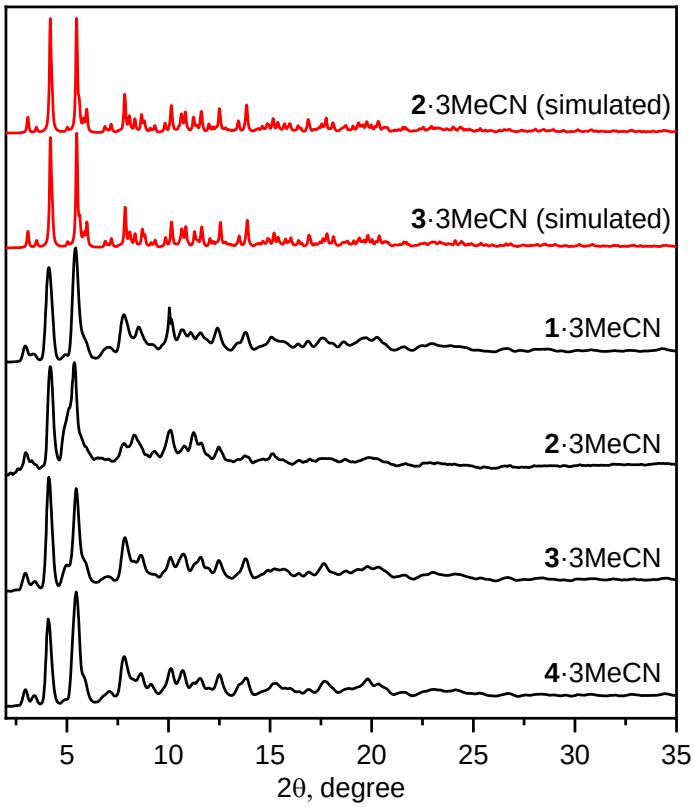

Figure S3. Simulated XRPD patterns of **2**·3MeCN and **3**·3MeCN (red) and experimental ones (black) of CPs (**1**−**4**)·3MeCN recorded at 150 K.

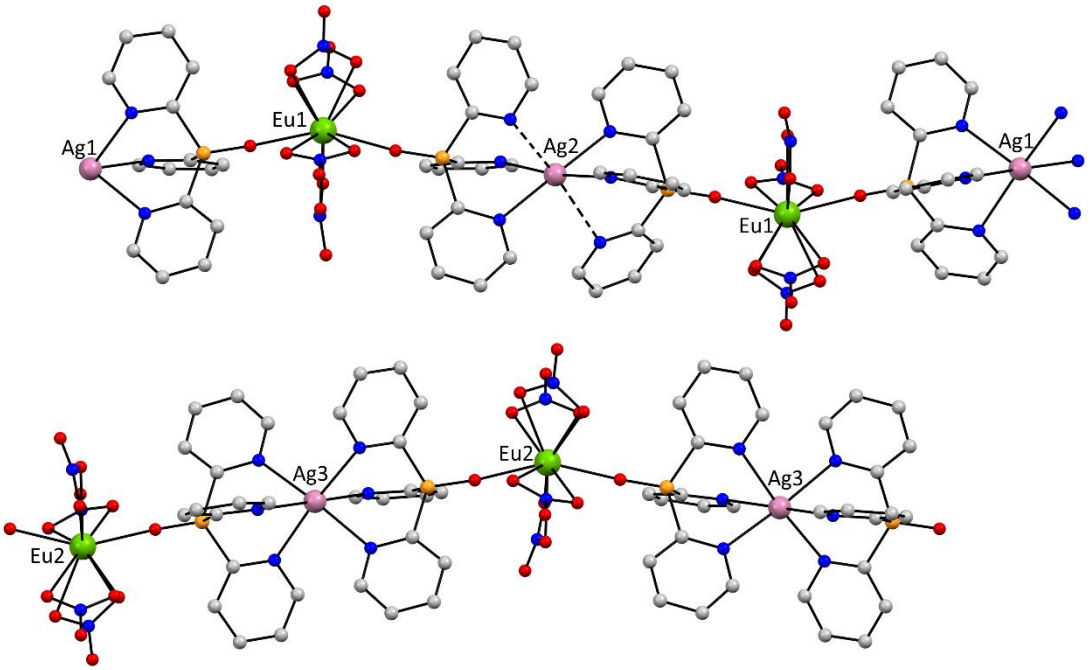

Figure S4. Fragment of the crystal structure of **2**·3MeCN. The longest Ag2–N bonds (d = 2.647 Å) are shown by dashed lines. H atoms, disordered atom positions, and solvent MeCN molecules are omitted for clarity. Color code: Eu, green; Ag, pink; C, grey; O, red; N, blue; P, orange.

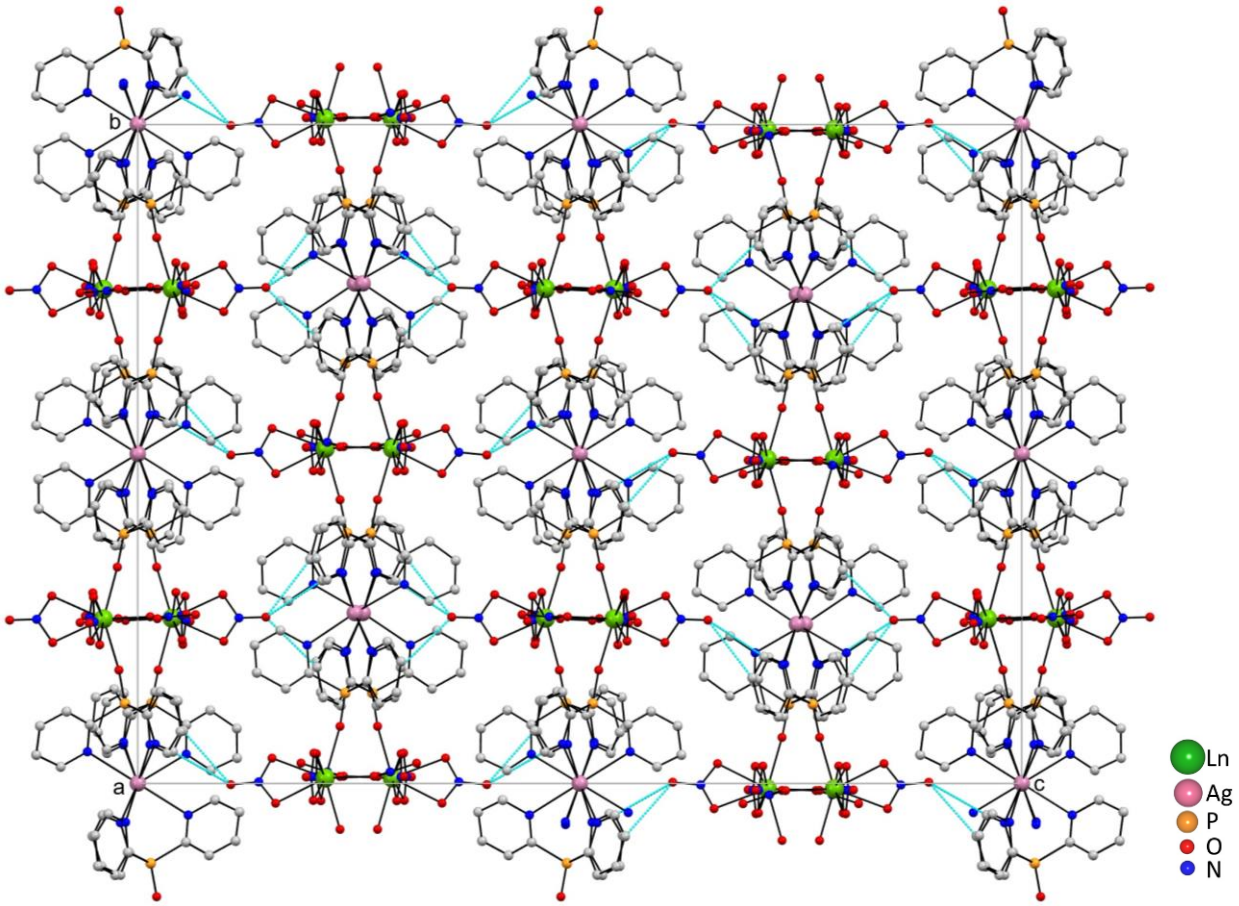

Figure S5. View of the crystal structure of **2**·3MeCN along the [100] direction. H atoms, disordered atom positions, and solvent MeCN molecules are omitted for clarity. Short contacts are shown in cyan.

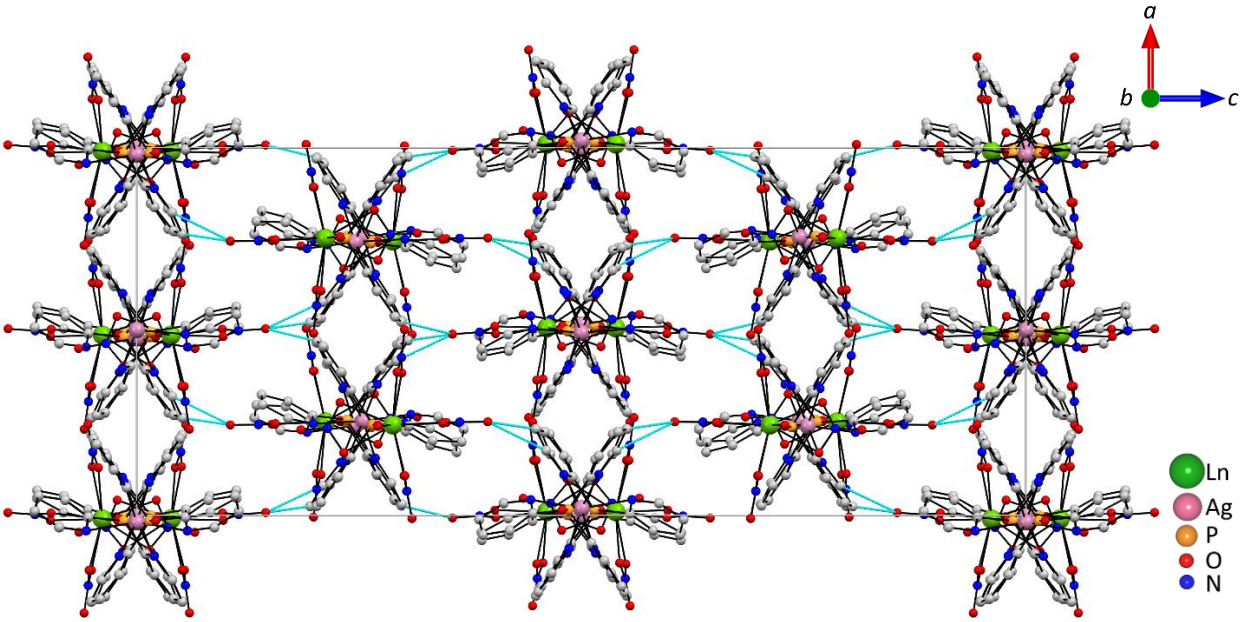

Figure S6. View of the crystal structure of **2**·3MeCN along the [010] direction. H atoms, disordered atom positions, and solvent MeCN molecules are omitted for clarity. Short contacts are shown in cyan.

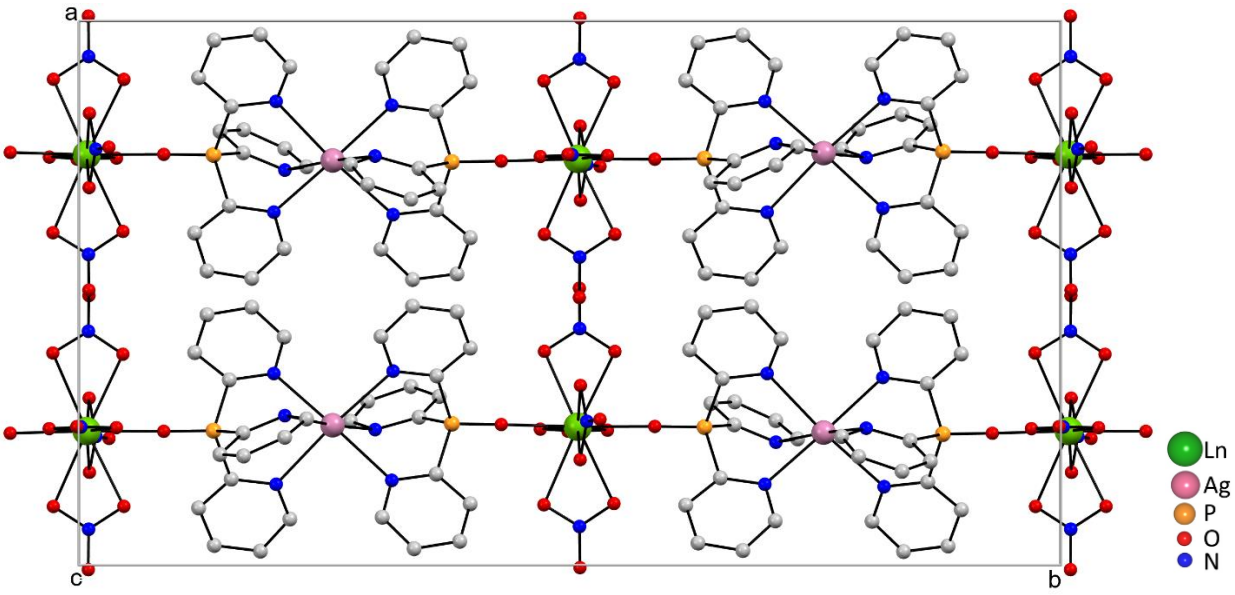

Figure S7. View of the crystal structure of **2**·3MeCN along the [001] direction. H atoms, disordered atom positions, and solvent MeCN molecules are omitted for clarity.

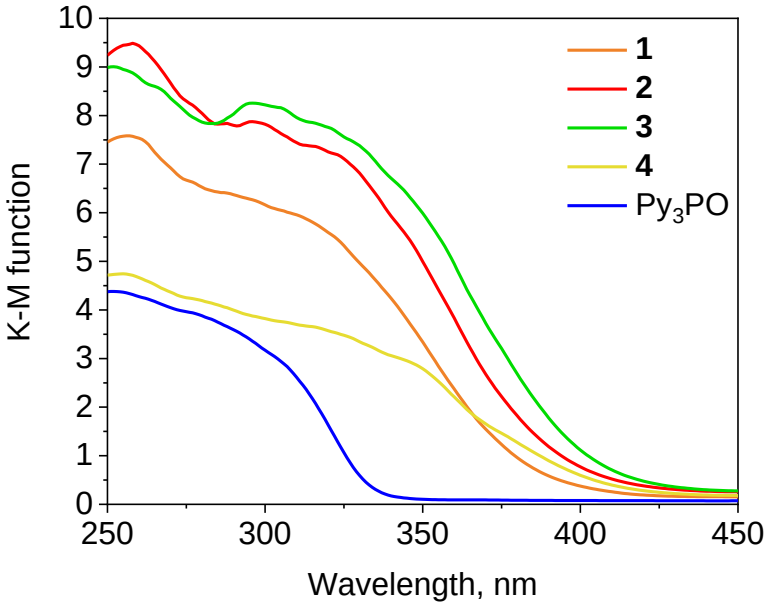

Figure S8. Diffuse reflectance spectra of CPs **1**–**4** and Py_3PO presented as Kubelka-Munk function *vs.* wavelength. All measurements were performed at room temperature.

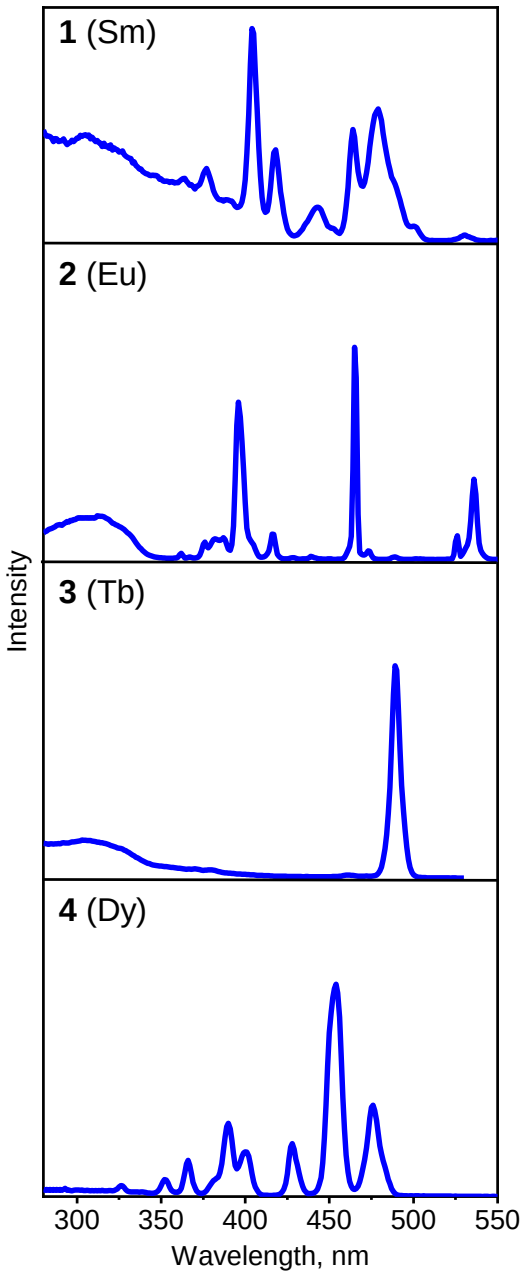

Figure S9. Normalized excitation spectra of CPs **1** (λ_{reg} = 640 nm), **2** (λ_{reg} = 615 nm), **3** (λ_{reg} = 545 nm), and **4** (λ_{reg} = 573 nm) in the solid state at 300 K**.**

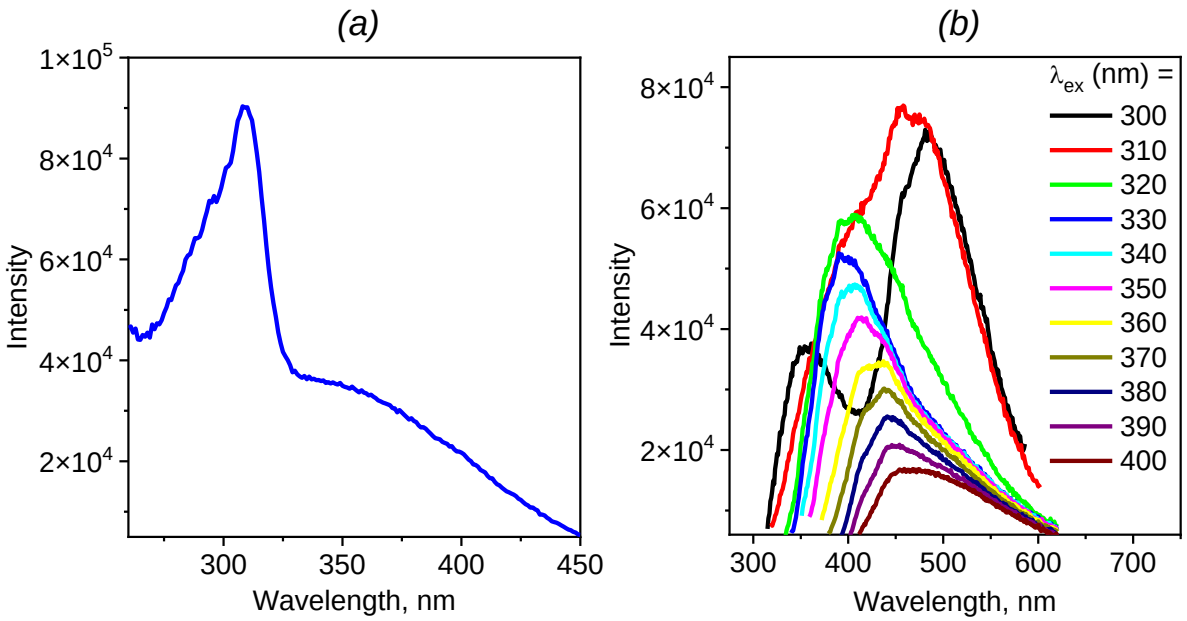

Figure S10. PL excitation spectrum at λ_{reg} = 480 nm (*a*) and emission spectra recorded at different excitation wavelengths (*b*) of Py_3PO in the solid state at 300 K.

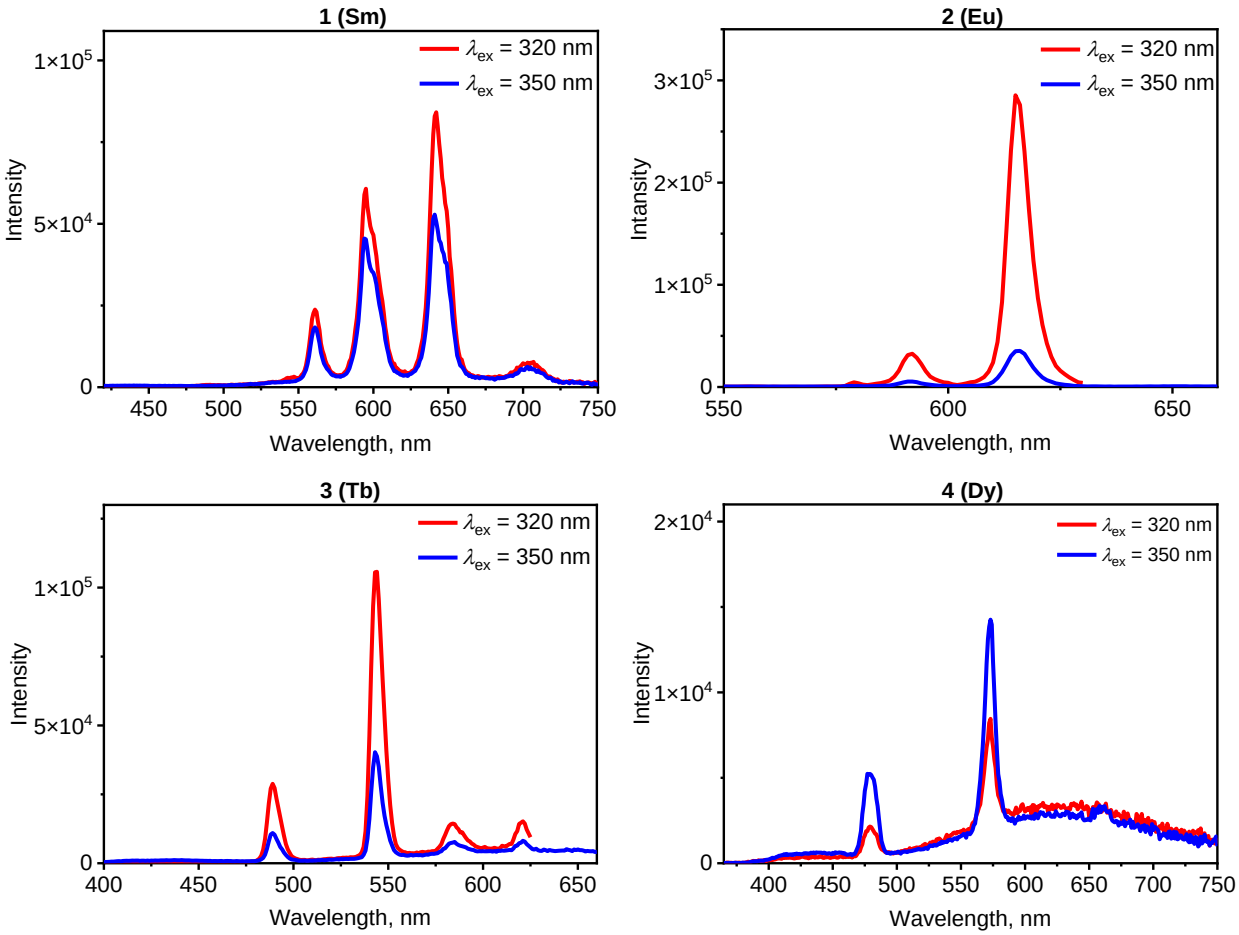

Figure S11. Emission spectra of CPs **1**–**4** recorded at λ_{ex} = 320 nm (red) and 350 nm (blue) in the solid state at 300 K**.**

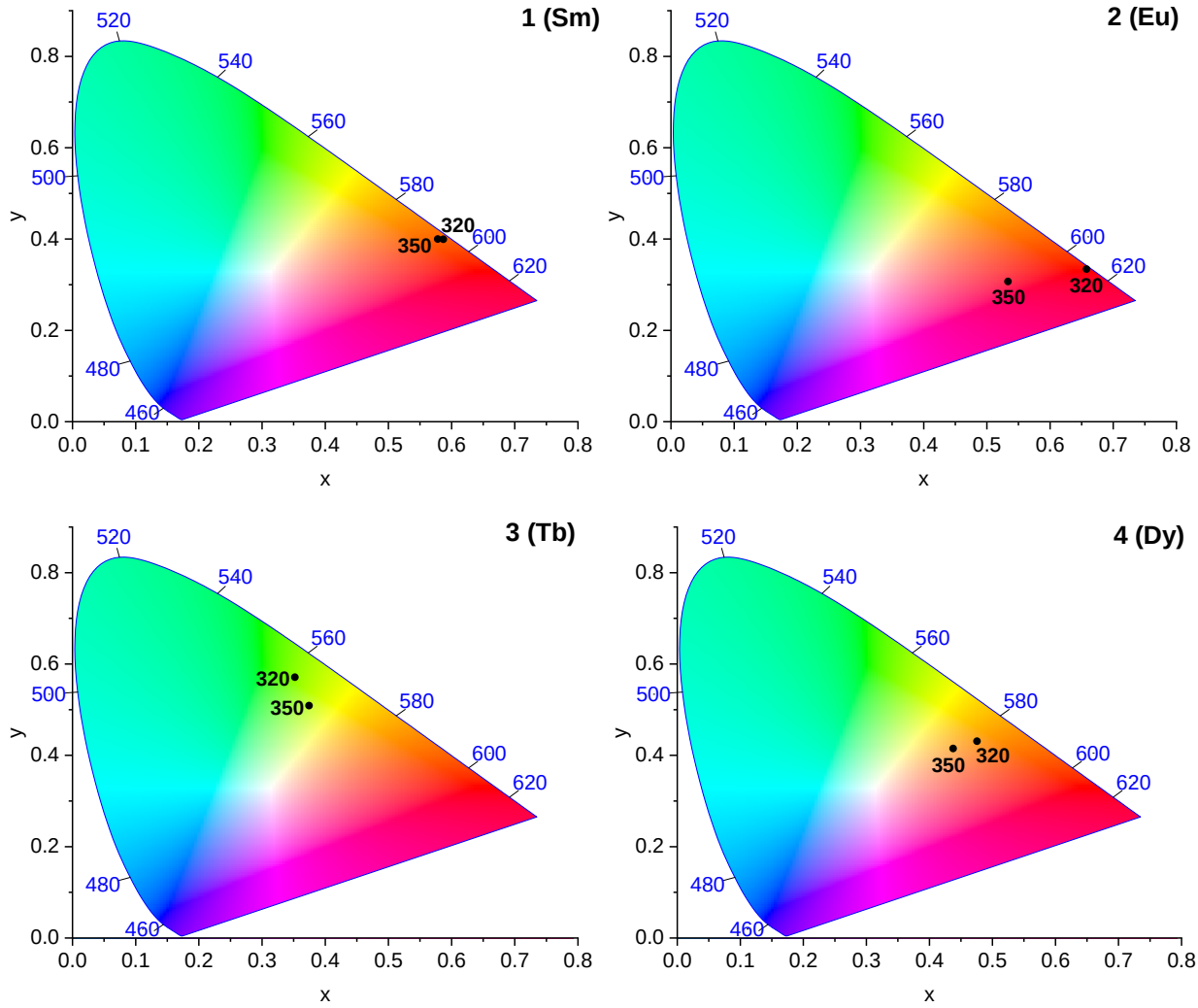

Figure S12. CIE 1931 chromaticity diagrams demonstrating dependence of the emission color of CPs **1**–**4** on the excitation wavelength.

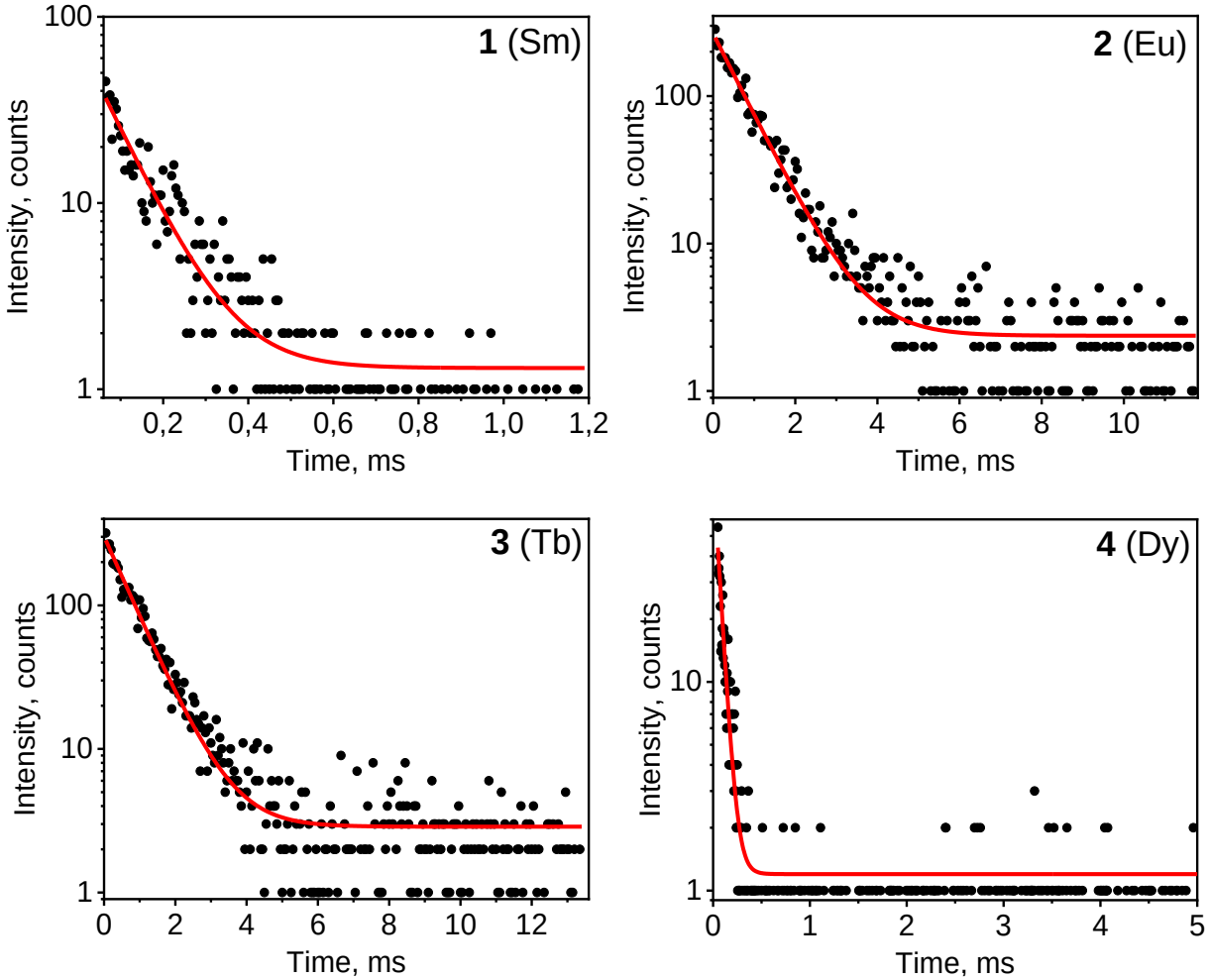

Figure S13. Kinetics of PL decay of CPs **1** (λ_{reg} = 640 nm), **2** (λ_{reg} = 615 nm), **3** (λ_{reg} = 545 nm), and **4** (λ_{reg} = 573 nm) in the solid state at 300 K. The PL was excited at 320 nm.

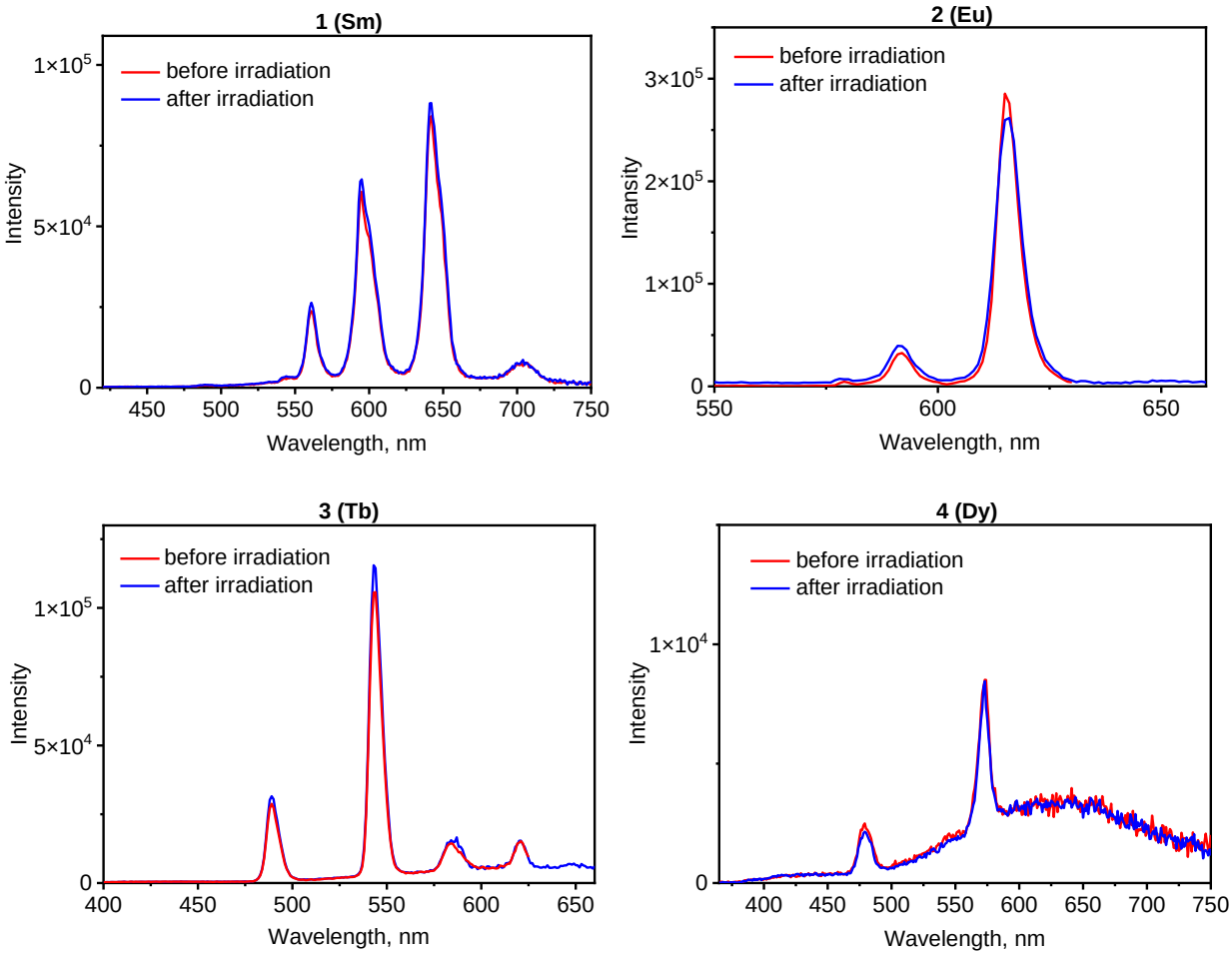

Figure S14. Emission spectra of CPs **1–4** before (red) and after (blue) irradiation at 312 nm for 3 hours recorded at λ_{ex} = 320 nm in the solid state at 300 K**.**